is analogous to an imine carbon and more importantly that C(3) (~47 ppm) is an sp^3-like carbon, which is different from that in a normal indole ring showing signals at ~100 ppm.[17b,18]

The spectrum of **1** isolated from CD_3OD exhibited almost no CH_2 signal (0.3 H), implying that the C(3) position is deuterated probably during the indole ⇌ 3*H*-indole interconversion with proton migration. Addition of pyridine to a methanol solution of **1** gave $Pd(py)_2Cl_2$ as crystals, whereas with added dimethyl-d_6 sulfoxide the NMR spectrum of **1** in $CDCl_3$ changed to that of free MI in 24 h. The results indicate that the Pd(II)-indole bond is weak and that MI resumes its normal indole structure upon dissociation as shown below:

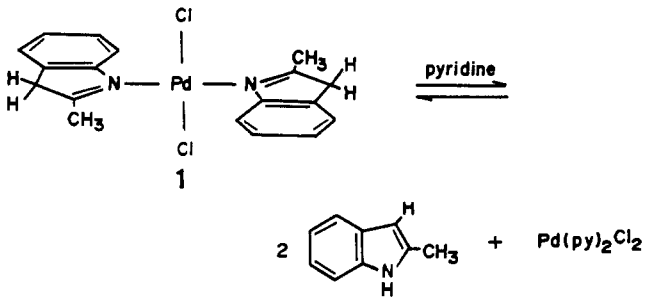

Transformation of the indole ring is also supported by the ultraviolet absorption spectra of **1** and **2** in $CHCl_3$ (Figure 4), where the indole peaks at ~270 and 280-295 nm are replaced with a broad band centered at a shorter wavelength without the characteristic shoulder peaks.[20] They exhibited a peak assignable to the d-d transition at 395 nm (ϵ = 170 M^{-1} cm^{-1}), which corresponds with the reflectance spectra of **1** and **2** showing maxima at 395 and 456-458 nm.

Concluding Remarks. The present findings offer evidence for the weak coordinating ability of the indole nitrogen and the intermediacy of the 3*H*-indole ring probably formed in the metal ion catalyzed reactions, and may explain the reactivities of indoles in such reactions.[2] In hydrophobic environments where the Lewis acidity of metal ions is stronger than in aqueous media, metal ions such as Cu(II) having a high affinity for nitrogens may be able to interact with the indole nitrogen in the manner observed for Pd(II), and this could be a possibility in biological systems.

Acknowledgment. We thank Takahiro Saito and Takayasu Yamazaki for assistance with the experiments. Thanks are also due to Kenzo Deguchi of JEOL for the measurements of ^{13}C-CP/MAS NMR spectra. This work was supported in part by a Grant-in-Aid for Scientific Research from the Ministry of Education, Science, and Culture of Japan, to which our thanks are due.

Supplementary Material Available: Tables of fractional coordinates and isotropic thermal parameters for non-hydrogen and hydrogen atoms, anisotropic thermal parameters for non-hydrogen atoms, bond lengths and angles and torsion angles for $[Pd(MI)_2Cl_2]$ and $[Pd(DMI)_2Cl_2]$ (3 pages). Ordering information is given on any current masthead page.

(18) Morales-Rios, M. S.; Espineira, J.; Joseph-Nathan, P. *Magn. Reson. Chem.* **1987**, *25*, 377-395.

(19) The assignment of the indole ring (C(2), C(3a), and C(7a)) and methyl (C(2m)) signals was further supported by the ^{13}C NMR spectrum obtained by the dipolar dephasing method.

(20) The ternary system containing Pd(II), L-glutamate, and tryptamine at pH 5.8 exhibited strong absorption peaks at 325 and 393 nm with ϵ = 2400 and 1920 $M(Pd)^{-1}$ cm^{-1}, respectively, and unusually intense circular dichroism peaks at 415 nm ($\Delta\epsilon$ = 4.55 $M(Pd)^{-1}$ cm^{-1}) and at 280 nm ($\Delta\epsilon$ = -5.33 $M(Pd)^{-1}$ cm^{-1}) corresponding to the indole ring absorption. A similar anomaly was also observed for 3-indoleacetate (unpublished results). Both could be related to the process of 3*H*-indole formation, its deprotonation, and/or metal binding at C(3) in 3*H*-indole.

Contribution from the School of Chemistry and Biochemistry, Georgia Institute of Technology, Atlanta, Georgia 30332-0400

Spectroelectrochemical Characterization of Nitridochromium(V) Porphyrins and Their Reactivity with Substituted Acetic Anhydrides

Lawrence A. Bottomley* and Frank L. Neely

Received May 31, 1989

The redox reactivity of a variety of nitridochromium(V) porphyrins was investigated by cyclic and differential pulse voltammetry as well as electronic and EPR spectroelectrochemical techniques. Each complex investigated underwent two single-electron reversible oxidation and two single-electron reversible reduction reactions at a Pt electrode in several nonaqueous solvents on the cyclic voltammetric time scale. The site of each electron-transfer reaction was centered on the porphyrin ring. This compares with the previously documented redox behavior of nitridomanganese(V) porphyrins but contrasts with the general redox behavior of chromium porphyrins. The reaction of nitridochromium(V) porphyrins with substituted acetic anhydrides produced (acylimido)chromium porphyrins at rates at least 1 order of magnitude faster than the corresponding nitridomanganese porphyrins. However, the subsequent transfer of the acylimido group from the Cr center to olefins was not observed for the complexes and olefins investigated herein. A spectroelectrochemical investigation revealed that the (acylimido)chromium porphyrins are best described as Cr(IV) cation radicals. This is in contrast to the corresponding (acylimido)manganese porphyrin complexes, which possess Mn(V) centers, and may account for the unreactivity of the (acylimido)chromium porphyrins with olefins.

In recent reports, we[1-3] and others[4-14] have detailed the unusual redox and functionalized nitrogen atom transfer reactivity of nitridomanganese porphyrins. Original interest in nitridomanganese porphyrins was spawned from the observation[4] that while high-valent manganese porphyrins are capable of oxidizing water, the high-valent nitridomanganese porphyrins are readily

(1) Bottomley, L. A.; Neely, F. L.; Gorce, J.-N. *Inorg. Chem.* **1988**, *27*, 1300-1303.

(2) Bottomley, L. A.; Luck, J. F.; Neely, F. L.; Quick, J. S. In *Redox Chemistry and Interfacial Behavior of Biological Molecules*; Dryhurst, G., Niki, K., Eds.; Plenum: New York, 1988; pp 77-86.

(3) Bottomley, L. A.; Neely, F. L. *J. Am. Chem. Soc.* **1988**, *110*, 6748-6752.

(4) Hill, C. L.; Hollander, F. J. *J. Am. Chem. Soc.* **1982**, *104*, 7318.

(5) Buchler, J. W.; Dreher, C.; Lay, K.-L. *Z. Naturforsch.* **1982**, *37B*, 1155-1162.

(6) Buchler, J. W.; Dreher, C.; Lay, K.-L. *Chem. Ber.* **1984**, *117*, 2261-2274.

(7) Buchler, J. W.; Dreher, C.; Lay, K.-L.; Lee, Y. A.; Scheidt, W. R. *Inorg. Chem.* **1983**, *22*, 888-891.

(8) Groves, J. T.; Takahashi, T. *J. Am. Chem. Soc.* **1983**, *105*, 2073.

(9) Buchler, J. W.; Dreher, C.; Lay, K.-L.; Raap, A.; Gersonde, K. *Inorg. Chem.* **1983**, *22*, 879-884.

(10) Buchler, J. W.; Dreher, C. *Z. Naturforsch.* **1984**, *39B*, 222-230.

(11) Groves, J. T.; Takahashi, T.; Butler, W. M. *Inorg. Chem.* **1983**, *22*, 884-887.

(12) Tsubaki, M.; Hori, H.; Hotta, T.; Hiwatashi, A.; Ichikawa, Y.; Yu, N.-T. *Biochemistry* **1987**, *26*, 4980-4986.

(13) Yamamoto, Y.; Imamura, T.; Suzuki, T.; Fujimoto, M. *Chem. Lett.* **1988**, 261.

(14) Takahashi, T. Ph.D. Dissertation, University of Michigan, 1985.

0020-1669/90/1329-1860$02.50/0

isolated. Our spectroelectrochemical investigation[1] of substituted nitridomanganese tetraphenylporphyrins revealed that nitridomanganese porphyrins can undergo two sequential and stepwise porphyrin ring oxidations or porphyrin ring reductions, with full retention of the nitrido group. Thus, the otherwise electroactive Mn central metal atom was deactivated via axial coordination by the nitride ligand.

The nitridomanganese group can be chemically activated toward functionalized nitrogen atom transfer reactivity. Groves[8] has shown that trifluoroacetic anhydride[15] reacts with NMn(TMP)[15] to form the acylimido complex, $[(CF_3C(O)N)Mn(TMP)]^+[O_2CCF_3]^-$. Upon subsequent treatment with cyclooctene, the nitrene added across the double bond to form the corresponding aziridine. In recent studies,[2,3] we have shown that the formation of the acylimido complex is the rate-determining step in the overall functionalized nitrogen atom transfer reaction and that this reaction can be generalized to a wide variety of manganese porphyrins. The rate of formation of the acylimido complex can be varied over 3 orders of magnitude and is dependent upon porphyrin ring basicity, the acetic anhydride substituent, and the steric environment about the nitrido–Mn reaction center.

Very recently, Woo[16] has shown that nitridomanganese porphyrins are capable of reversible nitrogen atom transfer with manganese(II) porphyrins. We have shown,[17] independently, that treatment of nitridomanganese porphyrins with chromium(III) porphyrins results in rapid, quantitative, and irreversible nitrogen atom transfer to the Cr center. Thus, nitridomanganese porphyrins display unusual nitrogen atom transfer reactivity involving both olefinic and metallic substrates. The latter is without precedent.

Hill[4] and Groves[11] have shown that the nitridochromium(V) porphyrins are structurally similar to their nitridomanganese(V) porphyrin counterparts. Both complexes possess pentacoordinate metal centers raised above the porphyrin plane toward the triply bonded axial nitride. Interestingly, Takahashi[14] has mentioned unsuccessful attempts to extend the functionalized nitrogen atom transfer reactivity of NCr(TMP) with olefins. His treatment of NCr(TMP) with TFAA produced the acylimido complex, but subsequent reaction with cyclooctene did not result in the formation of the corresponding aziridine at any appreciable rate.

In this account, we present a spectroelectrochemical characterization of the redox reactivity of nitridochromium(V) porphyrins and document our efforts to promote nitrogen atom transfer reactivity of NCr(POR) with olefins. In addition, we propose an explanation for the contrasting reactivity of (acylimido)chromium and (acylimido)manganese porphyrins with olefins based on our kinetic and spectral analysis of the reaction of a variety of nitridochromium(V) porphyrins with selected substituted acetic anhydrides.

Experimental Section

The nitridochromium(V) porphyrins[15] utilized in this study were prepared according to the procedure of Buchler[9] from the corresponding hydroxochromium(III) porphyrins. The hydroxochromium(III) porphyrins were prepared from the corresponding free-base porphyrins by Buchler's method.[9] The free-base porphyrins were synthesized from the appropriately substituted benzaldehyde and pyrrole via Adler's classic method.[24] The purity of all porphyrins was verified by UV–vis, NMR, and mass spectral measurements. Salient spectral features for all of the nitridochromium(V) porphyrins are summarized in the following listing. Peak maxima are listed in nm with the corresponding logarithm of the molar absorptivity in parentheses. NCr(T-2,4,6-$(OCH_3)_3$-PP): 428 (5.65), 546 (4.33). NCr(T-2,4-$(OCH_3)_2$-PP): 427 (5.65), 545 (4.31). NCr(T-2-OCH_3-PP): 427 (5.65), 544 (4.32). NCr(T-4-OCH_2Ph-PP): 427 (5.65), 543 (4.32). NCr(T-4-OCH_3-PP): 425 (5.65), 543 (4.38). NCr(T-4-CH_3-PP): 425 (5.62), 542 (4.35). NCr(TPP): 425 (5.64), 542 (4.38). NCr(T-4-F-PP): 422 (5.65), 542 (4.36). NCr(T-4-Cl-PP): 422 (5.64), 542 (4.36). NCr(T-4-CF_3-PP): 421 (5.62), 541 (4.33). NCr(T-4-CN-PP): 421 (5.61), 541 (4.30). NCr(OEP): 407 (5.48), 536 (4.11), 562 (4.45). The infrared spectrum of each of the nitridochromium(V) porphyrins contained the usual porphyrin vibrations. The Cr≡N stretching vibration was found in the range 1014–1018 cm^{-1}.

All reagents were obtained from Aldrich Chemical Co. and purified in the manner previously described.[16] The spectroelectrochemical instrumentation and techniques were identical with those previously reported.[18] The EPR experiments were performed on a Varian E3 spectrometer. All experiments were carried out at ambient temperature (21 ± 1 °C). Unless otherwise noted, all solutions were deoxygenated with solvent-saturated nitrogen and blanketed with nitrogen during all experiments. All potentials are referenced to the SCE.

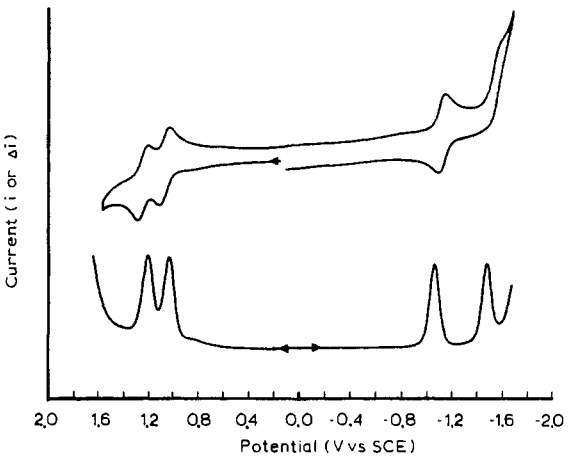

Figure 1. Voltammograms acquired on a 1.10 mM solution of NCr(TPP) in 0.1 M TBAP/DCE with a Pt-button electrode. The upper voltammogram is a cyclic voltammogram obtained at a potential sweep rate of 200 mV s^{-1}. The lower trace is a differential pulse voltammogram taken at a potential sweep rate of 20 mV s^{-1}, a pulse amplitude of 25 mV, and a pulse frequency of 0.1 s.

Table I. Half-Wave Potential Data[a] for the Electrode Reactions of Selected Nitridochromium(V) Porphyrins Dissolved in DCE

	redox reacn			
porphyrin	1	2	3	4
NCr(T-2,4,6-$(OCH_3)_3$-PP)	1.02	0.85	−1.27	−1.74
NCr(T-2,4-$(OCH_3)_2$-PP)	1.08	0.92	−1.18	−1.64
NCr(T-2-OCH_3-PP)	1.16	0.99	−1.17	−1.48
NCr(T-4-OCH_2Ph-PP)	1.13	0.97	−1.14	−1.47
NCr(T-4-OCH_3-PP)	1.16	0.98	−1.14	−1.44
NCr(T-4-CH_3-PP)	1.18	1.02	−1.10	−1.46
NCr(TPP)	1.23	1.04	−1.08	−1.43
NCr(T-4-F-PP)	1.26	1.09	−1.09	−1.43
NCr(T-4-Cl-PP)	1.33	1.12	−1.06	−1.38
NCr(T-4-CF_3-PP)	1.37	1.19	−0.93	−1.36
NCr(T-4-CN-PP)	1.47	1.24	−0.89	−1.35

[a] Potentials are listed in volts.

Results and Discussion

Electrochemical Characterization of Nitridochromium(V) Porphyrins. The electrochemistry of a variety of nitridochromium(V) tetraphenylporphyrins with a select group of phenyl

(15) Abbreviations: porphyrin dianion = $(POR)^{2-}$; nitrido[5,10,15,20-tetrakis(2,4,6-trimethoxyphenyl)porphinato]chromium(V) = NCr(T-2,4,6-OCH_3-PP); nitrido[5,10,15,20-tetrakis(2,4-dimethoxyphenyl)-porphinato]chromium(V) = NCr(T-2,4-OCH_3-PP); nitrido-[5,10,15,20-tetrakis(2-methoxyphenyl)porphinato]chromium(V) = NCr(T-2-OCH_3-PP)Cr; nitrido[5,10,15,20-tetrakis(4-benzyloxyphenyl)porphinato]chromium(V) = NCr(T-4-OCH_2Ph-PP); nitrido-[5,10,15,20-tetrakis(4-methoxyphenyl)porphinato]chromium(V) = NCr(T-4-OCH_3-PP); nitrodo[5,10,15,20-tetrakis(4-methylphenyl)porphinato]chromium(V) = NCr(T-4-CH_3-PP); nitrido[5,10,15,20-tetraphenylporphinato]chromium(V) = NCr(TPP); nitrido[5,10,15,20-tetrakis(4-fluorophenyl)porphinato]chromium(V) = NCr(T-4-F-PP); nitrido[5,10,15,20-tetrakis(4-chlorophenyl)porphinato]chromium(V) = NCr(T-4-Cl-PP); nitrido[5,10,15,20-tetrakis(4-cyanophenyl)porphinato]chromium(V) = NCr(T-4-CN-PP); nitrido[octaethylporphinato]-chromium(V) = NCr(OEP); trifluoroacetic anhydride = TFAA; trichloroacetic anhydride = TCAA; dichloroacetic anhydride = DCAA; chloroacetic anhydride = MCAA; acetic anhydride = AA; ferrocene = FC; saturated calomel electrode = SCE; 1,2-dichloroethane = DCE; benzonitrile = PhCN; Pyridine = py.

(16) Woo, K. L.; Goll, J. G. *J. Am. Chem. Soc.* **1989**, *111*, 3755.
(17) Bottomley, L. A.; Neely, F. L. *J. Am. Chem. Soc.* **1989**, *111*, 5955.
(18) Bottomley, L. A.; Deakin, M. R.; Gorce, J.-N. *Inorg. Chem.* **1984**, *23*, 3563.

Table II. Half-Wave Potential Data[a] for the Electrode Reactions of NCr(TPP) and NCr(OEP) in Several Nonaqueous Solvents

porphyrin	reacn no.[b]	solvent			
		CH_2Cl_2	DCE	PhCN	py
NCr(TPP)	1	1.24	1.23	1.24	*c*
	2	1.04	1.04	1.00	0.98
	3	−1.08	−1.08	−0.99	−0.99
	4	−1.43	−1.43	−1.48	−1.48
NCr(OEP)	1	1.21	1.22	1.21	*c*
	2	0.83	0.84	0.85	0.86
	3	−1.30	−1.31	−1.30	−1.25
	4	−1.64	−1.65	−1.66	−1.65

[a] Potentials (V) were measured in 0.1 M TBAP, referenced to the SCE, and are uncorrected for liquid junction potentials. [b] See indicated reaction in text for corresponding electrode reactant and product. [c] The electrode reaction was beyond the accessible potential window of the solvent-supporting electrolyte system.

ring substituents was investigated at a Pt electrode in four nonaqueous solvents. Figure 1 depicts cyclic and differential pulse voltammograms obtained for NCr(TPP) dissolved in DCE. These voltammograms are representative of the voltammograms observed for all NCr(POR) compounds studied. The results of variable-potential sweep rate cyclic voltammetric and variable-pulse amplitude differential pulse studies confirmed that all four processes observed within the solvent-supporting electrolyte potential window are best described as reversible single-electron-transfer reactions on the voltammetric time scale. The number of electrons involved in each step was verified by controlled-potential coulometry. Table I lists the half-wave potentials observed for the NCr(POR) complexes dissolved in DCE.

Similarly shaped voltammograms and variable-potential sweep rate trends were obtained when NCr(TPP) and NCr(OEP) were dissolved in CH_2Cl_2, PhCN, and py. The solvent dependence of the half-wave potentials for these complexes is given in Table II. The absence of strong solvent–Cr(V) axial interaction is inferred from the observation that the half-wave potentials for all four charge transfers are essentially unchanged from nonbonding (CH_2Cl_2 and DCE) to strongly bonding (py) solvents. This behavior is comparable to that previously observed for nitridomanganese porphyrins.[1]

Constant-potential chronoabsorptometric experiments were performed at an optically transparent thin-layer electrode. Figure 2A depicts the spectra acquired for NCr(TPP) dissolved in DCE after the potential of the electrode was stepped from 0.20 to 1.10 V. The spectrum of the reactant, characterized by an intense Soret band at 424 nm, diminished in intensity and was replaced by a broad, low-intensity Soret band centered at 442 nm. The spectral transition was complete within 30 s and occurred with isosbestic points at 402, 439, 527, and 560 nm. When the applied potential was reset to 0.20 V immediately following the oxidative electrolysis, the characteristic spectrum of the starting material was quantitatively regenerated. When the reset operation was delayed or when the solvent contained traces of H_2O, the observed spectrum was a mixture of that characteristic of the starting material and a Cr^{III} byproduct (Soret band at 451 nm and visible bands at 525, 562, and 602 nm). The intensity of the Cr^{III} byproduct band was directly proportional to the time delay prior to the potential reset.

During the course of the electrolysis in the cavity of an EPR spectrometer, the intense, eleven-line spectrum characteristic of Cr^{V} split by five N atoms gradually collapsed to a very broad line spectrum centered at $g = 2.002$. At longer electrolysis times, a nine-line pattern emerged. This spectrum was superimposable on the spectrum obtained on a sample of $[Cr^{III}(TPP)]^+$. Takahashi[14] has previously shown that $[NCr(TMP)]^+$ exhibits a broad-line EPR spectrum (at $g = 1.993$) at ambient temperature. In frozen CH_2Cl_2 at 108 K, the EPR spectrum indicates that the cation has rhombic symmetry; g values of 2.064, 1.995, and 1.944 were observed.

Figure 2B depicts the spectra acquired for NCr(TPP) dissolved in DCE after the potential of the electrode was stepped from −0.70 to −1.20 V. The spectrum of the reactant was replaced by a broad,

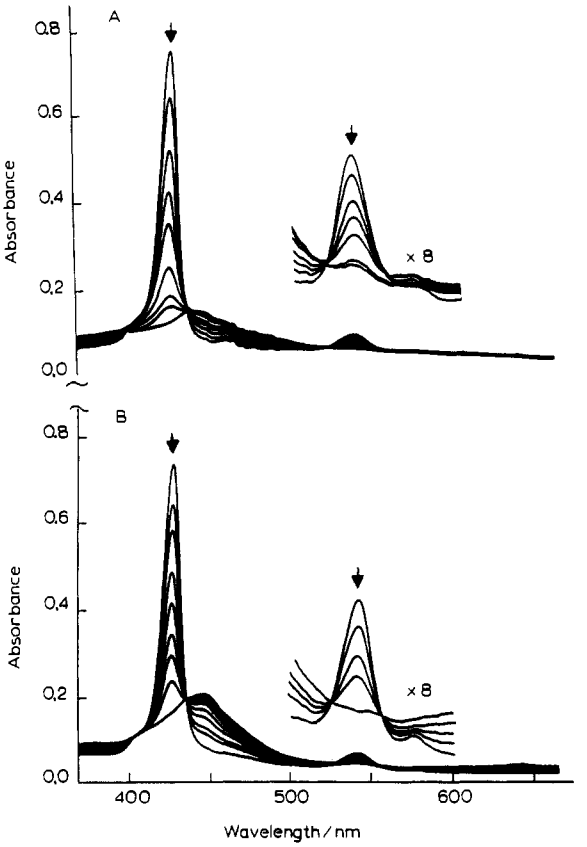

Figure 2. Electronic spectra acquired during the electrolysis of an 81 μM solution of NCr(TPP) in 0.2 M TBAP/DCE. In part A (the upper trace) the spectra were acquired following a potential step of the optically transparent electrode from 0.20 to 1.10 V. In part B (the lower trace) the spectra were acquired following the application of a potential step from −0.70 to −1.20 V.

low-intensity band at 447 nm. The visible band at 543 nm collapsed during the course of the reductive electrolysis, and two small peaks at 470 and 649 nm grew in intensity. Isosbestic points were observed at 439, 528, and 558 nm, indicating the absence of any long-lived intermediates. Immediate reapplication of the potential of the optically transparent electrode to −0.70 V regenerated the spectrum of the starting material in its entirety. At longer delay times, the spectrum obtained after reapplication of the −0.70 V potential was a mixture of NCr(TPP) and $[Cr^{III}(TPP)]^+$. The intensity of the Soret band of NCr(TPP) diminished and that of $[Cr^{III}(TPP)]^+$ increased in direct proportion to that time the electrode was held at −1.20 V.

The electrogeneration of the first reduction product was also accomplished in the cavity of an EPR spectrometer at ambient temperature. During the course of the electrolysis, the eleven-line spectrum characteristic of NCr(TPP) decayed to an EPR-silent spectrum. Continued application of the reductive potential gave rise to a low-intensity nine-line spectrum characteristic of $[Cr^{III}(TPP)]^+$ and indicating loss of the nitride. Upon reversal of the potential step back to −0.70 V, the eleven-line spectrum characteristic of NCr(TPP) was only partially reproduced and was overlapped with the nine-line Cr^{III} spectrum.

On the basis of the results presented above, the pathway detailed in reactions 1–4 is proposed for the electrode reactions of nitri-

$$[NCr^{V}(POR)]^{2+} + e^- \Leftrightarrow [NCr^{V}(POR)]^+ \quad (1)$$

$$[NCr^{V}(POR)]^+ + e^- \Leftrightarrow NCr^{V}(POR) \quad (2)$$

$$NCr^{V}(POR) + e^- \Leftrightarrow [NCr^{V}(POR)]^- \quad (3)$$

$$[NCr^{V}(POR)]^- + e^- \Leftrightarrow [NCr^{V}(POR)]^{2-} \quad (4)$$

dochromium(V) porphyrins on the voltammetric time scale. Justification of this electrode mechanism follows several lines of

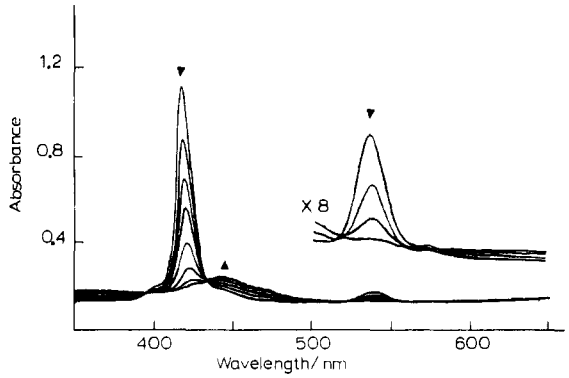

Figure 3. Electronic spectra acquired as a function of time after the addition of 2.0 μL of TFAA to 3.00 mL of 2.76 μM NCr(TPP) in DCE.

evidence. For the oxidation processes (reactions 1 and 2), the electronic spectrum of the electrode products possess broad Soret bands of diminished intensity and visible bands shifted to longer wavelengths. These spectral features have been shown to be characteristic of porphyrin cation radicals.[19] Secondly, the EPR spectra are consistent only with porphyrin-ring-centered reactions. The Cr(V) center in the NCr(POR) starting material has an electronic configuration of d^1. An EPR-silent material would be produced if the site of the oxidative charge transfer were metal centered. Thirdly, and IR spectrum obtained for a sample of NCr(TPP) oxidized by ferric perchlorate exhibited a strong band at 1280 cm^{-1}, indicative of a porphyrin cation radical. Fourthly, the potential difference between the first and second oxidations for all NCr(POR) complexes investigated is comparable to the theoretical values as well as to empirical values previously observed with the analogous NMn(POR) complexes.[1,20]

For the reduction processes (reactions 3 and 4), the site of charge transfer is also ring centered. The electronic spectra acquired for the reduction products were comparable to those of metalloporphyrin anion radicals.[19] Secondly, the potential difference between reactions 3 and 4 averaged 350 mV and the potential difference between reactions 2 and 3 (the band gap) averaged 2.11 V. These values compare favorably with those observed for NMn(POR) (357 mV and 2.075 V) as well as that predicted from molecular orbital calculations for redox reactions centered at the porphyrin ring.[18,20] Thirdly, the silent EPR spectrum acquired following the first reduction is consistent either with spin pairing of the Cr(V) d^1 electron with that of the porphyrin anion radical or with a Cr(IV) species possessing a low-spin d^2 electronic configuration. The analogous redox reaction for NMn(POR) (where the electronic configuration of the Mn center was d^2) produced an anion-radical species characterized by a single EPR resonance at $g = 2.017$.

Linear free energy relationships equating the half-wave potential for all four reactions of the various NCr(POR) complexes measured in DCE with the Hammett–Taft substituent constant were constructed in the usual fashion.[21] The computed ρ values were 0.064, 0.067, 0.050, and 0.077 V for reactions 1–4, respectively. The ρ values are about 10 mV greater than those observed for the analogous NMn(POR) complexes.[1] This observation is consistent with the general trend observed by Kadish that within the first-row transition-metal porphyrins, the ρ values increase with decreasing atomic number.[22] The ρ values obtained herein are comparable to values previously reported for porphyrin-ring-centered oxidations of chromium(III) porphyrins and virtually identical with those reported for the similarly substituted free-base porphyrins.[21,22] These comparisons lend additional credence to the assignment of porphyrin-ring-centered electron transfers.

Table III. Apparent Rate Constants[a] for the Reaction of Nitridochromium(V) Porphyrins with Substituted Acetic Anhydrides

	anhydride				
porphyrin	AA	MCAA	DCAA	TCAA	TFAA
NCr(T-4-OCH_3-PP)				1500	
NCr(T-4-CH_3-PP)				440	
NCr(TPP)	nr[b]	<0.1	2.8	170	>2000
NCr(T-4-F-PP)				91	
NCr(T-4-Cl-PP)				21	
NCr(OEP)	nr[b]	<0.1	3.4	830	>2000
NMn(OEP)	nr[b]	nr[b]	1.4	4.8	8.5

[a] Apparent rate constants are listed in $s^{-1} \times 10^4$. The precision of each entry in this table was within 5% relative standard deviation as determined from three replicates. [b] No reaction was observed after 4 h.

Reactions of Nitridochromium(V) Porphyrins. Figure 3 depicts the temporal dependence of the electronic spectrum of NCr(TPP) when treated with a 1000-fold excess of TFAA. The final spectrum has the appearance of a π-cation-radical spectrum with a low-intensity Soret band at 445 nm. When the time course of this reaction is followed by EPR, the eleven line spectrum characteristic of NCr(TPP) collapses to an EPR-silent spectrum. An infrared spectrum acquired on the reaction product possesses a strong band at 1270 cm^{-1}, diagnostic of a porphyrin π cation radical. Furthermore, carbonyl stretches at 1681 and 1709 cm^{-1} attributable to the imido carbonyl and TFA anion, respectively, were present as intense bands in the infrared spectrum. The corresponding vibrations of the [(trifluoroacyl)imido]Mn(TPP) derivative were measured at 1695 and 1743 cm^{-1}, respectively. The acylimido complex could be converted back to NCr(TPP) by addition of a slight excess of tetra-*n*-butylammonium hydroxide (dissolved in DCE) to solutions containing the complex. The progress of the acylimido complex decomposition was readily monitored by electronic and EPR spectroscopy. Similar spectral results and reactivity trends were obtained for the reaction of NCr(OEP) or the substituted tetraphenylporphyrins with the substituted acetic anhydrides MCAA, DCAA, and TCAA.

The kinetics of the formation of the (acylimido)chromium porphyrin complex were determined from the temporal dependence of the absorbance of both the Soret and visible bands of the nitridochromium(V) reactant. First-order kinetics were observed over the ranges 2.5 μM [porphyrin] < 50 μM and 1.0 mM < [substituted acetic anhydride] < 1000 mM. These conditions were identical with those used for the NMn(POR) study. The apparent rate constants are given in Table III. For comparison, k_{app} values for NMn(OEP) are also listed in this table. No reaction was observed for acetic anhydride after waiting 4 h. On the other hand, the reaction of both NCr(OEP) and NCr(TPP) with TFAA was complete during the time interval of mixing (less than 10 s). The relative rate of the reaction decreased in the order TFAA > TCAA > DCAA > MCAA. Treatment of any of the acylimido complexes with a 10-fold excess of olefin (cyclooctene, norbornylene, or 1-hexene) produced no detectable aziridine or $[Cr^{III}(POR)]^+$ after 4 h.

The formation of (acylimido)chromium porphyrins proceeds via nucleophilic attack of the nitride on the electron-deficient carbonyl carbon of the anhydride. The dependence of the rate constants on the acetic anhydride substituents is consistent with this mechanism. Secondly, the k_{app} values for the reaction of NCr(OEP) with either TCAA or DCAA were larger than the values observed for the analogous reaction with NCr(TPP). The increased rate of NCr(OEP) mirrors the increased basicity of OEP as compared to TPP and, thus, the nucleophilicity of the reaction center. Thirdly, for the series of para-substituted tetraphenylporphyrins, the log of the ratio k(NCr(T-4-Z-PP))/k(NCr(TPP)) (where Z denotes a non-hydrogen phenyl ring substituent) was linearly related to the Hammett–Taft substituent parameter, suggesting a uniform mechanism over this series. A ρ value of −0.95, roughly twice that previously observed for NMn(T-4-Z-PP),

(19) (a) Carnieri, N.; Harriman, A. *Inorg. Chim. Acta* **1982**, *62*, 103. (b) Wollberg, A.; Manassen, J. *J. Am. Chem. Soc.* **1970**, *92*, 2982. (c) Gans, P.; Marchon, J. C.; Reed, C. A.; Regnard, J. R. *Nouv. J. Chim.* **1981**, *5*, 203.
(20) Kadish, K. M. *Prog. Inorg. Chem.* **1987**, *34*, 435 and references therein.
(21) Bottomley, L. A.; Olson, L.; Kadish, K. M. In *Electrochemical and Spectrochemical Studies of Biological Redox Components*; Kadish, K. M., Ed.; American Chemical Society: Washington, DC, 1982; Chapter 13 and references therein.
(22) Kadish, K. M.; Morrison, M. M. *Bioelectrochem. Bioenerg.* **1977**, *3*, 480.

Table IV. Half-Wave Potential Data[a] for the Products of the Reaction of TFAA with Selected Para-Substituted NCr(TPP) Complexes

porphyrin	oxidn	redn
(T-4-OCH_2Ph-PP)	1.10	0.66
(T-4-OCH_3-PP)	1.11	0.69
(T-4-CH_3-PP)	1.16	0.70
(TPP)	1.22	0.74
(T-4-F-PP)	1.23	0.76
(T-4-Cl-PP)	1.28	0.77

[a] Potentials (V) were measured in DCE that was 0.1 M in TBAP, referenced to the SCE, and are uncorrected for liquid junction potentials.

was obtained. Fourthly, the k_{app} values for reactions of NMn(OEP) with TFAA and TCAA were substantially less than the values obtained for the corresponding reactions of the chromium porphyrins. X-ray crystallographic determinations have shown that the Mn≡N core is displaced from the center of the porphyrin by 38.8 pm whereas the Cr≡N core in NCr(T-4-CH_3-PP) is displaced toward the nitrido moiety by 42.1 pm.[4,11] Thus, the Cr≡N reaction center has greater exposure as compared to that of the Mn≡N reaction center and, hence, faster rates.

The reaction of NCr(POR) with substituted acetic anhydrides was also monitored electrochemically. Prior to the addition of the anhydride, the rest potential of the electrochemical cell was 0.05 V. Initiating cyclic voltammetric sweeps from this point gave two reversible oxidations and two reversible reductions characteristic of NCr(POR); vide supra. Addition of as little as a 3-fold excess of TFAA, TCAA, or DCAA resulted in an immediate shift in the rest potential to 0.95 V. Cyclic voltammetric sweeps initiated from this potential gave one oxidation and one reduction process. The reduction of free anhydride obscures the observation of any processes occurring at potentials negative of 0.0 V. The formation of the (acylimido)chromium porphyrin occurred too rapidly to observe any intermediates with cyclic voltammetry.

Variable-temperature and variable-potential sweep rate experiments were undertaken to determine the electron-transfer mechanism for each process. For the oxidation, the peak potential separation ($E_{p,a} - E_{p,c}$) as well as the peak symmetry ($E_{p,a} - E_{p,a/2}$) remained essentially constant at 60 mV over the potential sweep rate range 20–1000 mV s^{-1}. The peak current ratio was 0.80 at a potential sweep rate of 500 mV s^{-1} and decreased with decreasing sweep rate. In addition, the value of $i_{p,a}/v^{1/2}$ decreased with decreasing sweep rate. These trends were consistent with theory for an electron-transfer reaction complicated by a following chemical reaction. Voltammograms recorded at ambient temperature with potential sweep rates faster than 1 V s^{-1} or at temperatures lower than 0 °C at all potential sweep rates were devoid of the complication of the following chemical reaction.

The passage of one electron per molecule was confirmed by integration of the charge passed during several exhaustive electrolysis experiments. Electrolyses carried out at an optically transparent thin-layer electrode held at a potential of 1.40 V produced nonisosbestic electronic spectral changes. The final spectrum was featureless over the range 350–650 nm. Reapplication of a potential of 0.90 V did not result in the regeneration of the visible spectrum characteristic of the (acylimido)chromium porphyrin and confirmed the existence of a following chemical reaction. An identical experiment performed in the cavity of an EPR spectrometer gave no observable EPR spectrum throughout the course of the electrolysis. Interestingly, the oxidation potential was found to be invariant with anhydride identity but was markedly dependent upon the identity of the phenyl ring substitutent as listed in Table IV. A ρ value of 80 mV was found for the oxidation process. Therefore, we have tentatively assigned this electron-transfer reaction as a porphyrin-ring-centered processes.

The reduction of the (acylimido)Cr(TPP) complexes was studied in a similar manner as described above for the oxidation. The results of variable-potential sweep rate and variable-temperature studies confirmed that the reduction is also a one-electron-transfer process with a following chemical reaction. The reduction process becomes chemically uncomplicated when carried out at temperatures below −20 C. Controlled-potential electrolyses carried out at 0.60 V resulted in isosbestic changes in the visible spectrum. The Soret band of the (trifluoroacylimido)Cr(TPP) complex at 445 nm reduced in intensity and was replaced by a sharp, intense band at 456 nm. New bands were observed at 531, 569, and 604 nm. The spectrum of the ultimate product of the reduction was identical with that of (TFA)Cr(TPP). When the potential was stepped back to the rest potential, the Soret band at 456 nm collapsed to give a broad, diffuse spectrum that did not resemble that of [(trifluoroacyl)imido]Cr(TPP). This behavior confirms the assignment of the reduction process as an EC process.

Similar results were obtained for the (trichloroacyl)- and (dichloroacyl)imido complexes. The midpoint potentials gave a slight dependence on anhydride identity: 0.74 V for TFAA, 0.73 V for TCAA, and 0.71 V for DCAA. The ρ value obtained for the potential dependence on phenyl ring substitutent was 61 mV, comparable to the values obtained for the electrode reactions of NCr(POR). We have tentatively assigned the reduction as a porphyrin-ring-centered reaction, formally generating an unstable Cr(IV) species.

The voltammetric behavior of (acylimido)Cr(POR) complexes contrasts with that of the corresponding (acylimido)Mn(POR) complexes. The voltammetric fingerprint of NMn(POR) is very similar to that of NCr(POR), i.e. two single-electron oxidations and two single-electron reductions. Formation of (acylimido)-Mn(POR) following addition of anhydride to solution is detected by a positive potential shift for both oxidation processes.

On the basis of the spectral and electrochemical characteristics cited above, the product of the reaction of NCr(POR) with substituted anhydride is best formulated as an (acylimido)Cr(IV) cation-radical species. Since (acylimido)Cr(POR) complexes are unreactive with cyclooctene, norbornene, or 1-hexene, the Cr(IV) center must be a better electrophile for the nitrene than for the olefins. Attempts to facilitate functionalized nitrogen atom transfer by electrooxidizing the coordinated nitrenoid Cr(IV) cation radical in the presence of a 10-fold excess of cyclooctene were unsuccessful. The unreactivity of either the (acylimido)-Cr(POR) or the oxidized (acylimido)Cr(POR) complexes contrasts with the reactivity of oxochromium(IV) porphyrins with olefins[23] but is consistent with the preference of the nitrene for the more electrophilic Cr(IV) center compared to that of the olefin. We are currently investigating the reactions of other Mn and Cr macrocyclic compounds with substituted acetic anhydrides. With these, we hope to prepare (acylimido)metal(V) complexes that will readily undergo functionalized nitrogen atom transfer when treated with olefins.

Acknowledgment. Support of this research by the Department of Health and Human Services through the National Institute of Heart and Lung via Grant No. HL-33734 is gratefully acknowledged.

Registry No. [NCr(T-2,4,6-$(OCH_3)_3$-PP)]$^+$, 126422-84-2; [NCr(T-2,4,6-$(OCH_3)_3$-PP)], 126457-23-6; [NCr(T-2,4,6-$(OCH_3)_3$-PP)]$^-$, 126423-00-5; [NCr(T-2,4,6-$(OCH_3)_3$-PP)]$^{2-}$, 126423-11-8; [NCr(T-2,4-$(OCH_3)_3$-PP)]$^+$, 126422-85-3; [NCr(T-2,4-$(OCH_3)_3$-PP)], 126422-93-3; [NCr(T-2,4-$(OCH_3)_3$-PP)]$^-$, 126423-01-6; [NCr(T-2,4-$(OCH_3)_3$-PP)]$^{2-}$, 126423-12-9; [NCr(T-2-OCH_3-PP)]$^+$, 126457-21-4; [NCr(T-2-OCH_3-PP)], 126457-24-7; [NCr(T-2-OCH_3-PP)]$^-$, 126423-02-7; [NCr(T-2-OCH_3-PP)]$^{2-}$, 126423-13-0; [NCr(T-4-OCH_2Ph-PP)]$^+$, 126422-86-4; [NCr(T-4-OCH_2Ph-PP)], 126422-94-4; [NCr(T-4-OCH_2Ph-PP)]$^-$, 126423-03-8; [NCr(T-4-OCH_2Ph-PP)]$^{2-}$, 126423-14-1; [NCr(T-4-OCH_3-PP)]$^+$, 126422-87-5; [NCr(T-4-OCH_3-PP)], 126422-95-5; [NCr(T-4-OCH_3-PP)]$^-$, 126423-04-9; [NCr(T-4-OCH_3-PP)]$^{2-}$, 126457-25-8; [NCr(T-4-CH_3-PP)]$^+$, 126422-88-6; [NCr(T-4-CH_3-PP)], 84174-28-7; [NCr(T-4-CH_3-PP)]$^-$, 126423-05-0; [NCr(T-4-CH_3-PP)]$^{2-}$, 126423-15-2; [NCr(TPP)]$^+$, 126422-89-7; [NCr(TPP)], 84174-79-8; [NCr(TPP)]$^-$, 126423-06-1; [NCr(TPP)]$^{2-}$, 126423-16-3; [NCr(T-4-F-PP)]$^+$, 126457-22-5; [NCr(T-4-F-PP)], 126422-96-6; [NCr(T-4-F-PP)]$^-$,

(23) Bruice, T. C. *Aldrichimica Acta* **1988**, *21*, 87–94.
(24) Adler, A. D.; Longo, F. R.; Finarelli, J. D.; Goldmacher, J.; Assour, J.; Korsakov, L. *J. Org. Chem.* **1967**, *32*, 476.

126423-07-2; $[NCr(T\text{-}4\text{-}F\text{-}PP)]^{2-}$, 126423-17-4; $[NCr(T\text{-}4\text{-}Cl\text{-}PP)]^{+}$, 126422-90-0; $[NCr(T\text{-}4\text{-}Cl\text{-}PP)]$, 126422-97-7; $[NCr(T\text{-}4\text{-}Cl\text{-}PP)]^{-}$, 126423-08-3; $[NCr(T\text{-}4\text{-}Cl\text{-}PP)]^{2-}$, 126423-18-5; $[NCr(T\text{-}4\text{-}CF_3\text{-}PP)]^{+}$, 126422-91-1; $[NCr(T\text{-}4\text{-}CF_3\text{-}PP)]$, 126422-98-8; $[NCr(T\text{-}4\text{-}CF_3\text{-}PP)]^{-}$, 126423-09-4; $[NCr(T\text{-}4\text{-}CF_3\text{-}PP)]^{2-}$, 126423-19-6; $[NCr(T\text{-}4\text{-}CN\text{-}PP)]^{+}$, 126422-92-2; $[NCr(T\text{-}4\text{-}CN\text{-}PP)]$, 126422-99-9; $[NCr(T\text{-}4\text{-}CN\text{-}PP)]^{-}$, 126423-10-7; $[NCr(T\text{-}4\text{-}CN\text{-}PP)]^{2-}$, 126423-20-9; $[NCr(OEP)]^{+}$, 126423-22-1; $[NCr(OEP)]$, 84174-29-8; $[NCr(OEP)]^{-}$, 126423-23-2; $[NCr(OEP)]^{2-}$, 126541-09-1; $(CF_3CC(O)N)Mn(TPP)$, 126423-21-0; NMn(OEP), 84206-82-6; AA, 108-24-7; MCAA, 541-88-8; DCAA, 4124-30-5; TCAA, 4124-31-6; TFAA, 407-25-0; $(T\text{-}4\text{-}OCH_2Ph\text{-}PP)$, 17260-17-2; $(T\text{-}F\text{-}OCH_3\text{-}PP)$, 22112-78-3; $(T\text{-}4\text{-}CH_3\text{-}PP)$, 14527-51-6; (TPP), 917-23-7; (T-4-F-PP), 37095-43-5; (T-4-Cl-PP), 22112-77-2; nitride, 18851-77-9.

Contribution from the Department of Chemistry, Southwest Texas State University, San Marcos, Texas 78666, and Department of Chemical and Biological Sciences, Oregon Graduate Institute of Science and Technology, Beaverton, Oregon 97006-1999

Resonance Raman Spectra of High- and Low-Spin Ferric Phenolates. Models for Dioxygenases and Nitrile Hydratase

Carl J. Carrano,*[1a] Mary W. Carrano,[1a] Kamala Sharma,[1b] Gabriele Backes,[1b] and Joann Sanders-Loehr*[1b]

Received August 30, 1989

A series of ferric phenolate complexes with Schiff base or methylamine substitutents ortho to the phenolic oxygen have been investigated. These include complexes with *N,N'*-ethylenebis((*o*-hydroxyphenyl)glycine), e.g., Na[Fe(EHPG)]; *N*-[2-(*o*-salicylideneamino)ethyl](*o*-hydroxyphenyl)glycine, e.g., $[Fe(EHGS)(X)_n]$, where $(X)_n = OH^-$, H_2O, or $(CN^-)_3$; and N^1,N^4-disalicylidenetriethylenetetramine, e.g., $[Fe((sal)_2trien)](PF_6)$. Although the majority of the complexes contained high-spin Fe(III), two low-spin species were generated: $[Fe((sal)_2trien)](PF_6)$ at 90 K and $[Fe(EHGS)(CN)_3]^{3-}$. Upon excitation within the phenolate → Fe(III) CT band, the resonance Raman spectra of both the high- and low-spin complexes are dominated by a set of phenolate vibrational modes at approximately 615, 630, 895, 1120, 1280, 1330, 1450, 1475, 1560, and 1600 cm^{-1}. The Schiff base containing ligands exhibit an additional resonance-enhanced vibration due to $\nu(C{=}N)$ at ~1640 cm^{-1}. The approximate doubling in the number of resonance-enhanced modes compared to the number in the Raman spectra of iron tyrosinate proteins is a consequence of the lower symmetry of ortho- relative to para-substituted phenolates. A correlation between Fe–O(phenolate) bond length with the intensity and/or frequency of the ~600-cm^{-1} Fe–O stretching mode is proposed to explain the variability in the energy and intensity of the ν(Fe–O) mode in iron tyrosinate proteins. The primary consequence of the formation of a low-spin state is to shift the phenolate → Fe(III) CT band from ~480 to ~650 nm, on the basis of the corresponding shift in the enhancement maximum of the ferric phenolate vibrational modes.

Introduction

Iron tyrosinate proteins are now recognized as a distinct class of nonheme proteins, which includes the transferrins, the purple acid phosphatases, and a number of aromatic ring cleaving dioxygenases.[2,3] These proteins all contain high-spin Fe(III) characterized by a $g = 4.3$ EPR signal and a strong absorption band in the 400–600-nm range (ϵ_M = 2000–4000 M^{-1} cm^{-1}) due to a phenolate oxygen to iron charge-transfer (CT) transition. In addition, these proteins show characteristic resonance-enhanced phenolate vibrations which have proven to be a useful resonance Raman (RR) signature. More recently a subclass of these iron–tyrosinate proteins has been discovered that have low-spin Fe(III) in their active sites. This group includes the tricyano adduct of transferrin[4] and the dicyano adduct of protocatechuate 3,4-dioxygenase.[5] Comparison with several low-spin iron(III) phenolate model complexes, $[Fe(EHGS)(CN)_3]^{3-}$ and the low-temperature form of $[Fe((sal)_2trien)]^{+}$ (Figure 1), shows that the low-spin species are characterized by small magnetic moments ($\mu_{eff} \simeq 2.0\ \mu_B$), anisotropic $g \simeq 2$ EPR spectra, and absorption bands in the 600–750-nm range ($\epsilon_M \simeq 1000$).[6-8a] The enzyme nitrile hydratase has similar EPR (g values of 2.28, 2.14, and 1.97) and electronic absorption (λ_{max} at 712 nm, ϵ_M = 1400 per Fe) properties,[8b] indicating that this protein may also belong to the low-spin iron(III) tyrosinate category.[6]

The 600–750-nm absorption band that is associated with low-spin complexes has been assigned as phenolate → Fe(III) CT on the basis of optical electronegativity arguments.[6] However, direct evidence for this assignment has been lacking. For this reason, a number of high- and low-spin ferric phenolate complexes have been examined by resonance Raman spectroscopy. We have found a similar set of iron phenolate modes in both cases, but with some shift in frequencies and intensities for the low-spin complexes. The enhancement of intensities with red excitation shows that the visible absorption bands in low-spin iron phenolates are indeed phenolate oxygen to iron CT transitions and that resonance Raman spectroscopy provides a unique spectral signature which may be useful in identifying low-spin Fe(III) sites in iron proteins.

Experimental Procedures

The ligands for the Fe(III) complexes used in this study are depicted in Figure 1. The meso and rac isomers of Na[Fe(EHPG)] were prepared and purified as previously described.[9a] The isomeric purity was checked by thin-layer chromatography on silica gel using the upper layer of a butanol/H_2O/acetic acid (4:5:1) mixture. The aquo and hydroxo complexes of Fe(EHGS) were also prepared by published procedures.[9b,10]

(1) (a) Southwest Texas State University. (b) Oregon Graduate Institute of Science and Technology.
(2) Que, L., Jr. In *Biological Applications of Raman Spectroscopy*; Vol. 3, Spiro, T. G., Ed.; Wiley: New York, 1988; Vol. 3, pp 491–521.
(3) (a) Harris, D. C.; Aisen, P. In *Iron Carriers and Iron Proteins*; Loehr, T. M., Ed.; VCH: New York, 1989; pp 239–351. (b) Sanders-Loehr, J. *Ibid.*, pp 373–466. (c) Que, L., Jr. *Ibid.*, pp 467–524.
(4) Swope, S. K.; Chasteen, N. D.; Weber, K. E.; Harris, D. C. *J. Am. Chem. Soc.* **1988**, *110*, 3835.
(5) Whittaker, J. W., Lipscomb, J. D. *J. Biol. Chem.* **1984**, *259*, 4487.
(6) Spartalian, K.; Carrano, C. J. *Inorg. Chem.* **1989**, *28*, 19.
(7) Tweedle, M. F.; Wilson, L. J. *J. Am. Chem. Soc.* **1976**, *98*, 4824.
(8) (a) Sakurai, H.; Tsuchiya, K.; Migita, K. *Inorg. Chem.* **1988**, *27*, 3877. (b) Sugiura, Y.; Kuwahara, J.; Nagasawa, T.; Yamada, H. *J. Am. Chem. Soc.* **1987**, *109*, 5848.
(9) (a) Patch, M. G.; Simolo, K. P.; Carrano, C. J. *Inorg. Chem.* **1983**, *22*, 2630. (b) Carrano, C. J.; Spartalian, K.; Appa Rao, G. V. N.; Pecoraro, V. L.; Sundaralingam, M. J. *J. Am. Chem. Soc.* **1985**, *107*, 1651.

0020-1669/90/1329-1865$02.50/0